

Beta adrenoceptor blockade ameliorates impaired glucose tolerance and alterations of the cerebral ceramide metabolism in an experimental model of ischemic stroke

Sebastian Luger, Annette Schwebler, Rajkumar Vutukuri, Nerea Ferreiros Bouzas, Sandra Labocha, Yannick Schreiber, Robert Brunkhorst, Helmuth Steinmetz, Josef Pfeilschifter and Waltraud Pfeilschifter 

Ther Adv Neurol Disord

2018, Vol. 11: 1–17

DOI: 10.1177/
1756286418769830

© The Author(s), 2018.
Reprints and permissions:
[http://www.sagepub.co.uk/
journalsPermissions.nav](http://www.sagepub.co.uk/journalsPermissions.nav)

Abstract

Background: Sphingolipids are versatile signaling molecules derived from membrane lipids of eukaryotic cells. Ceramides regulate cellular processes such as proliferation, differentiation and apoptosis and are involved in cellular stress responses. Experimental evidence suggests a pivotal role of sphingolipids in the pathogenesis of cardiovascular diseases, including ischemic stroke. A neuroprotective effect has been shown for beta-adrenergic antagonists in rodent stroke models and supported by observational clinical data. However, the exact underlying pathophysiological mechanisms are still under investigation. We aimed to examine the influence of propranolol on the ceramide metabolism in the stroke-affected brain.

Methods: Mice were subjected to 60 or 180 min transient middle cerebral artery occlusion (tMCAO) and infarct size, functional neurological deficits, glucose tolerance, and brain ceramide levels were assessed after 12, 24, and 72 h to evaluate whether the latter two processes occur in a similar time frame. Next, we assessed the effects of propranolol (10 mg/kg bw) at 0, 4 and 8 h after tMCAO and FTY720 (fingolimod; 1 mg/kg) on infarct size, functional outcome, immune cell counts and brain ceramide levels at 24 h after 60 min tMCAO.

Results: We found a temporal coincidence between stroke-associated impaired glucose tolerance and brain ceramide accumulation. Whereas propranolol reduced ischemic lesion size, improved functional outcome and reduced brain ceramide accumulation without an effect on circulating immune cells, FTY720 showed the known neuroprotective effect and strong reduction of circulating immune cells without affecting brain ceramide accumulation.

Conclusions: Propranolol ameliorates both stroke-associated impairment of glucose tolerance and brain ceramide accumulation which are temporally linked, strengthening the evidence for a role of the sympathetic nervous system in regulating post-stroke glucose metabolism and its metabolic consequences in the brain.

Keywords: stroke, glucose metabolism, hyperglycemia, ceramides, sphingolipids, FTY720, beta blockade

Received: 26 November 2017; revised manuscript accepted: 12 March 2018.

Introduction

Stroke is the third leading cause of death worldwide and the leading cause of long-term disability in western countries.¹ Therefore, a better understanding of the pathophysiological mechanisms of this highly prevalent disease is necessary in order to further optimize treatment strategies.

Currently, experimental evidence suggesting a pivotal role of sphingolipids in the pathogenesis of cardiovascular diseases, including ischemic stroke, is accumulating. Sphingolipids, signaling molecules derived from sphingomyelin, a component of cell membranes, play an important role in intracellular and receptor-mediated signal

Correspondence to:
Waltraud Pfeilschifter
Department of Neurology,
Goethe University,
Neurovascular Lipid
Signalling Group (NLSG),
Schleusenweg 2–16,
Frankfurt am Main, 60528,
Germany
w.pfeilschifter@med.uni-frankfurt.de

Sebastian Luger
Robert Brunkhorst
Department of Neurology,
Goethe University,
Frankfurt am Main,
Germany; Institute of
General Pharmacology
and Toxicology, Goethe
University, Frankfurt am
Main, Germany

Annette Schwebler
Helmuth Steinmetz
Department of Neurology,
Goethe University,
Frankfurt am Main,
Germany

Rajkumar Vutukuri
Josef Pfeilschifter
Institute of General
Pharmacology and
Toxicology, Goethe
University, Frankfurt am
Main, Germany

Nerea Ferreiros Bouzas
Sandra Labocha
Yannick Schreiber
Institute of Clinical
Pharmacology, Goethe
University, Frankfurt am
Main, Germany

transduction in health and disease states. Of this class of signaling molecules, ceramides regulate pleiotropic cellular processes such as proliferation, differentiation, senescence and apoptosis and are involved in cellular stress responses, for example secondary to ischemia.² In particular, several different animal models of ischemia/reperfusion injury have shown that ceramide accumulation in ischemic tissue might be a crucial trigger of apoptosis. Endogenous ceramides are generated compartment-specifically in the plasma membrane, the endoplasmic reticulum, the Golgi apparatus and in mitochondria.² Regarding the latter site, various studies have suggested a close interplay between ceramide signaling, mitochondrial function and cell viability.^{3,4}

Mitochondrial dysfunction is a hallmark of cell death in ischemia/reperfusion injury. In particular, it has been proposed that ceramide accumulation in mitochondria leads to mitochondrial dysfunction by inducing the production of reactive oxygen species causing the disruption of the electron transport chain, the discharge of the mitochondrial transmembrane potential and the release of pro-apoptotic mitochondrial proteins.^{3,5} However, hitherto the time profile and the mechanisms of ceramide generation in response to ischemic stroke are poorly characterized.

Endogenous ceramides are generated by three different biochemical pathways, both in an anabolic and catabolic manner: ceramides can be produced *via* the so called *de novo* pathway involving several catalytic steps. At first, L-serine and palmitoyl-CoA are condensed to 3-ketosphinganine *via* L-serine palmitoyltransferase. Then 3-ketosphinganine is reduced by 3-ketosphinganine-reductase to generate sphinganine. N-acylation of sphinganine by ceramide synthase leads to the formation of dihydro-ceramide, which is finally converted to ceramide.⁶

It is known that six types of ceramide synthases exist in mammals, and that each of them attaches a specific length of fatty acyl-CoA to long chain bases.⁷ Therefore, ceramides can be classified in long chain (C14:0/C16:0/C18:0) and very long chain (C20:0/C22:0/C24:0) ceramides, due to their different length of fatty acyl-CoA residues after N-acylation of sphingosine.

In addition to the *de novo* pathway, ceramide can also be formed *via* the salvage pathway by

re-acylation of sphingoid long chain bases, such as sphingosin. This method of ceramide generation relies upon the reverse activity of the enzyme ceramidase (CDase).⁶ Finally, through a catabolic pathway, ceramides can be generated through hydrolysis of complex sphingolipids.^{7,8}

Apart from the local ischemic tissue damage, there is ample evidence that ischemic stroke also causes severe systemic reactions, affecting the homeostasis of the immune system and causing severe metabolic alterations that in turn may contribute to a worse clinical outcome. These 'distant effects' have been shown to be mediated by brain-derived cytokines and danger-associated molecular patterns (DAMPs), which are released into the systemic circulation.⁹ Recently, the importance of an activation of T-lymphocytes in the periphery for the early exacerbation of ischemic injury has been emphasized. The immunomodulatory sphingosine 1-phosphate analog FTY720 (fingolimod), which induces lymphopenia by preventing the egress of lymphocytes from lymph nodes in the periphery, has been shown by several independent groups to reduce ischemic lesion size and to improve functional outcome in the acute and recovery phase after stroke.^{10–12}

In addition to the immunological alterations, a well-known metabolic phenomenon in the context of acute stroke is the development of post-stroke hyperglycemia.¹³ Possible explanations for this observation include brain injury-induced activation of the hypothalamus–pituitary–adrenal (HPA) axis triggering serum glucocorticoid release and activation of the sympathetic nervous system resulting in catecholamine-mediated systemic hyperglycemia.^{14,15} However, in ischemic brain damage glucose has dual roles in cerebral energy metabolism and oxidative stress. On the one hand, ischemia itself is deleterious for the brain, since the brain heavily relies on a constant supply of oxygen and glucose to maintain its normal function whereas other tissues can alternatively quickly switch to metabolize fatty acids, amino acids and ketone bodies instead of glucose. On the other hand, accumulating experimental evidence indicates detrimental effects of post-stroke hyperglycemia exacerbating ischemic neuronal damage by various mechanisms: In animal models of cerebral ischemia/reperfusion, increased glucose delivery during the reperfusion phase was suggested to be accompanied by pronounced production of reactive oxygen species in

the ischemic tissue.¹⁶ Reactive oxygen species are relevant mediators of ischemic brain injury. Especially after restoration of blood flow, detrimental reactive oxygen species, such as superoxide, are generated in an oxygen-dependent manner by donation of glucose-derived reducing equivalents to molecular oxygen. This process is strongly glucose-dependent since glucose is the source for many reducing equivalents passing through the mitochondrial electron transport chain.¹⁷

Also in an animal model of tissue plasminogen activator-induced intracerebral hemorrhage, a causal relationship between hyperglycemia-induced production of superoxides, blood–brain barrier damage and the extent of hemorrhage has been suggested.¹⁸ Moreover, other animal experiments indicated a hyperglycemia-mediated disturbance of the cerebral microcirculation and increased blood–brain barrier disruption.¹⁹

Consequently, a mutually reinforcing pathophysiological link between both detrimental effects, post-stroke hyperglycemia and cerebral ceramide accumulation, might be a ceramide-induced and glucose-dependent production of reactive oxygen species in the mitochondria leading to exacerbation of ischemic brain damage.

This is translationally relevant since observational clinical studies show an association of increased blood glucose levels after stroke with increased mortality and poor functional recovery. However, hitherto no randomized control trial could show a clinical benefit from intensified blood glucose management in the treatment of acute ischemic stroke.²⁰

The aims of this study were the parallel characterization of the kinetics of post-stroke hyperglycemia and the temporal regulation of the cerebral ceramide metabolism in the acute phase of ischemic stroke. In a second step, we investigated the effect of two different pharmacological interventions on (1) the development of post-ischemic hyperglycemia, (2) the alteration of ceramide metabolism in the ischemic brain tissue, and (3) the development of the ischemic lesion size and functional outcome in experimental stroke. One of the two interventions was the beta-adrenergic antagonist propranolol to target the sympathetic autonomic nervous system and its potentially detrimental effects in the context of acute stroke.

The other was treatment with FTY720 which, besides its immunomodulatory effects,^{10–12} has been shown to reduce ceramide generation *via* the *de novo* pathway by inhibiting ceramide synthases.^{21,22} We hypothesized that treatment with FTY720 might also reduce cerebral ceramide accumulation in the ischemic brain tissue, thereby possibly mediating an alternative way of neuroprotection independently of its immune cell-directed actions.

Materials and methods

Animals

For all experiments, male C57BL/6 mice (strain J, 11–12 weeks, mean 26.1 g range 21.0–28.3 g, Charles River Laboratories, Sulzfeld, Germany) were used according to the National Institute of Health Guide for the Care and Use of Laboratory Animals (NIH Publications No. 80–23, revised 1996). All experiments were approved by the local governmental authorities (Regierungspraesidium Darmstadt, approval number F143/65). ARRIVE guidelines were considered to rise the reproducibility and quality of the data.

Sample size calculation and exclusion criteria

Sample size calculation was based upon clinical observations in humans assuming a post-stroke blood glucose increase from physiological values of about 100 mg/dl to around 180 mg/dl¹³ with a standard deviation of 30%. To detect this difference with a power (1– β) of 0.8 and a level of acceptability of a false positive result (α) of 0.05, a sample size of seven animals per group was required. Due to a relevant drop-out rate, mainly in the groups with long observation time (72 h) and severe cerebral ischemia [3 h of transient middle cerebral artery occlusion (tMCAO)], the intended sample size was not met in all of the experimental groups (Supplemental Table 1).

The following exclusion criteria were predefined: mice with a subarachnoid hemorrhage (SAH) or death due to SAH were excluded from further analysis. Mice which were found dead before the end of the respective observation period were excluded regarding ischemic lesion size and tandem mass spectrometry (LC-MS/MS) analyses. A further exclusion criterion was death not related to cerebral ischemia. Hence, every mouse which died of an unknown cause received a complete

autopsy. Mice that died within the respective observation period were included in the functional outcome analysis after subarachnoid hemorrhage (SAH) was ruled out. They were given the worst possible neuro-score in the functional outcome analysis.

Experimental model of middle cerebral artery occlusion. For the experiments with pharmacological interventions, the surgeons (SL and AS) were blinded to the drug (propranolol or FTY720 *versus* saline) pretreatment and sham and control animals were alternately operated. Mice were randomly assigned to the treatment groups regarding duration of tMCAO (60 *versus* 180 min), observation period (12, 24 or 72 h) and drug pretreatment.

Right tMCAO for 60 or 180 min was achieved as described previously.²³ In brief, surgery was performed under anesthesia with 1.5% isoflurane (Forene TM, Abbott, Wiesbaden, Germany) and 0.1 mg/kg buprenorphine (Temgesic TM, Essex Pharma, Munich, Germany) under spontaneous respiration. Focal cerebral ischemia was induced after a midline cervical incision and exposure of the right carotid bifurcation by introducing a standardized silicone-coated monofilament with a tip diameter of 0.23 mm (Doccol, Redlands, CA, USA) and advancing it along the internal carotid artery until the tip occluded the proximal stem of the middle cerebral artery. At 60 min or 180 min after induction of ischemia, the filament was withdrawn to initiate reperfusion. Control animals underwent the same operation procedure up to the exposure of the internal carotid artery to avoid cerebral ischemia (sham operation). Animals were sacrificed after 12, 24 or 72 h after the initiation of ischemia. Directly following the intervention, all animals received regular drinking water and food without restrictions.

Pharmacological interventions with propranolol and FTY 720. Propranolol [(±)-propranolol hydrochloride, Sigma-Aldrich], was dissolved in 0.9% sodium chloride solution and administered 10 mg/kg intra peritoneally (i.p.) at 0, 4 and 8 h after tMCAO as previously described.²⁴ The control animals were treated with sodium chloride 0.9% (saline) i.p. at the corresponding time points.

FTY720 (Cayman Chemicals) was dissolved in 0.9% sodium chloride solution (saline) at a final concentration of 10 µg/100 µl for i.p. injection.

FTY720 (1 mg/kg) was administered i.p. after the initiation of anesthesia as previously described.¹⁰ The control animals were treated with corresponding volumes of saline i.p. All treatments were administered by RV, who was not involved in the tMCAO operation and further sample processing and analyses.

Oral glucose tolerance test and blood glucose measurements. Glucose tolerance was determined by means of an oral glucose tolerance tests (OGTT). The tMCAO and sham-operated mice were fasted for 12 h before performing OGTT. Glucose syrup (Accu-Chek® Dextrose O.G-T, Roche Diagnostics, Mannheim, Germany) was administered *via* oral gavage (2 g/kg body weight). Blood samples (about 0.6–1 µl) were obtained from the tail vein right before and 0, 30, 60, 120 and 180 min after glucose intake. Blood glucose concentration in mg/dl was measured using the Accu-Chek® Aviva test system.

Assessment of the neurological deficit. A neurological examination was performed at the end of the respective observation period (12 h, 24 h or 72 h) using the modified Bederson score (Bederson and colleagues)²⁵ and the grip test for functional assessment in the rodent stroke model (Supplemental Table 2).²⁶ The modified Bederson score evaluates walking behavior, hemiparesis and resistance to lateral push on a scale between 0 to 5. The grip test evaluates the ability of the mice to clutch to a wooden bar on a scale of 5 to 0. For the grip test, the mice were placed carefully on a wooden bar (8 mm diameter) 20 cm above the ground until they attained firm grip. The time period to fall off was recorded with a maximum of 60 s. Mice were not trained before. The neurological examinations were videotaped and the assessment was performed in a blinded fashion (RB and WP). Mice that died within the observation period were assessed per protocol and given the worst outcome score in both functional outcome analyses.

Volumetry of ischemic lesion size. Animals were sacrificed 12, 24, or 72 h under deep anesthesia and perfused transcardially with saline solution. Brains were harvested and sliced using a mice brain matrix (ASI Instruments, Warren, USA) generating brain slices of 1 mm thickness, which were stained with 2% 2,3,5-triphenyltetrazolium chloride (TTC; Merck KgaA, Darmstadt, Germany) in phosphate buffered saline (PBS; pH 7.4)

for 10–15 min at 37°C as described previously.¹⁴ TTC is processed to a red dye by vital mitochondria, whereas unstained, white tissue represents the definite brain infarct. After staining, brain slices were positioned between transparent foils and front and back surfaces of the slices were scanned using a flatbed color scanner (CanoScan LiDE 100; Canon, Tokyo, Japan; settings: 600 dpi, full color).

Volumetry of the ischemic lesion, the contra- and the ipsilesional hemisphere was performed using a previously established automated ImageJ macro (ImageJ software, National Institutes of Health, Bethesda, USA).²⁷ Lesion size was corrected for edema by multiplying the infarct volume by the ratio of the contralateral to the ipsilateral hemisphere volume.

Determination of sphingolipid concentration in brain tissue by LC-MS/MS. Animals were sacrificed 12, 24, or 72 h after induction of focal cerebral ischemia. After perfusion, cortical samples of the brain tissue were immediately shock frosted in fluid nitrogen and stored at –80°C. The measurement of the cerebral ceramide species (ng/mg brain tissue) was performed by LC-MS/MS as described previously in detail.^{28,29}

Flow cytometry analysis of blood cell counts. With capillaries [microtubes, flushed with ethylenediaminetetraacetic acid (EDTA)], about 40 µl of blood were drawn from the facial vein of each animal per group (1 mg/kg bodyweight FTY720 *versus* saline) 24 h after surgical intervention. Each blood sample was immediately transferred to a Falcon tube with ice-cold 15 ml RPMI-1640 cell culture medium with 100 µl of EDTA (0.5 molar, pH 8). Falcon tubes were centrifuged for 7 min at 1000 rpm, 4°C and the supernatant was discarded. Erythrocytes were lysed with red cell lysis buffer (8.3 g NH₄Cl in 0.01 mol/l Tris-HCl, pH 7.4). After washing with RPMI, samples were incubated with FACS buffer (1% fetal calf serum in PBS/0.01% NaN₃) and the respective antibodies for 30 min. Samples were analyzed on a BD FACSCanto II (BD Biosciences, Heidelberg, Germany). The following fluorescently labeled anti-mouse monoclonal antibodies (BD Pharmingen, Heidelberg, Germany) were used: CD4 (cat. no. 553052, T-helper cells), CD8a (cat. no. 560469, cytotoxic T-cells), CD11b (cat. no. 557396, macrophages), CD11c (cat. no. 550261, dendritic cells), CD45 (cat. no. 553089, B-cells).

Statistical analyses. Prism 7 (GraphPad Software, La Jolla, CA, USA) was used for statistical analysis. Results are expressed as means ± standard deviation (SD). Statistical significance was assessed either with Student's *t* test for unpaired two-group analyses or a one-way analysis of variance (ANOVA) with Bonferroni correction for multigroup comparisons. Neuroscore data are given as median and range and depicted in a dot plot. Statistical significance was assessed using a Mann–Whitney test with Gaussian approximation. Mice that died within the observation period were assessed per protocol and given the worst outcome score in both functional outcome analyses. To analyze the time kinetics of cerebral ceramide species a linear regression model was used comparing slopes and calculating a *p*-value (two-tailed) testing the null hypothesis that the slopes are identical. With a *p*-value ≤0.5 it was concluded that slopes were significantly different. R² was chosen as a measure of goodness of fit.

Results

Ischemic lesion size in the time course of up to 72 h after 60 min and 180 min of tMCAO

A tMCAO of longer duration (3 h *versus* 1 h) leads to significantly larger infarct volumes 24 h (*p* = 0.005) after induction of focal cerebral ischemia. The 12 h and 72 h observation cohort showed similar trends (Figure 1).

Kinetics and profile of ceramide species in the ischemic cerebral cortex after focal cerebral ischemia

Focal cerebral ischemia led to an increase of ceramide species in the ischemic cerebral cortex in comparison with the respective sham-operated control group; an increase was found for both long chain (C16:0) and very long chain (C20:0, C24:0) ceramides. Notably, C14:0 ceramide was exclusively detectable in the ischemic cortex, whereas in the nonischemic control brain samples it was not present at relevant concentrations. This ischemia-induced increase was also found for dihydro-ceramides, which are direct precursors of ceramide in the *de novo* pathway of ceramide synthesis (Figure 2). Using a linear regression model, we also found a significant time-dependent increase over an observation period of 12, 24, and 72 h after both 1 h and 3 h of tMCAO for the following ceramide and dihydro-ceramide species:

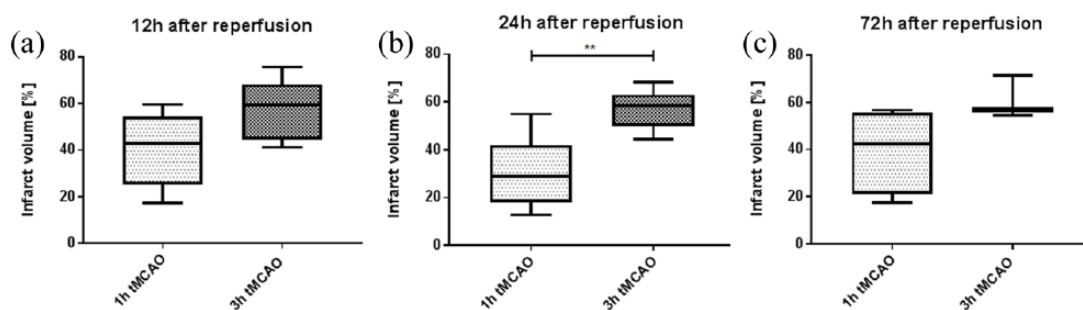


Figure 1. A tMCAO of longer duration (3 h *versus* 1 h) leads to a significant increase of infarction volume 24 h after induction of focal cerebral ischemia [24 h post-tMCAO: 1 h tMCAO $n = 5$; 3 h tMCAO $n = 6$; Figure 1(b)]. After an observation period of 12 h resp. 72 h there was a trend towards larger infarct volumes [12 h post-tMCAO: 1 h tMCAO $n = 5$; 3 h tMCAO $n = 7$; 72 h post-tMCAO: 1 h tMCAO $n = 4$; 3 h tMCAO $n = 3$]. The box boundaries mark the 25th and 75th percentile, the line within the box indicates the mean. Whiskers above and below the box mark the minimum and maximum. Statistical significance was assessed with Student's t test, $**p = 0.005$. tMCAO, transient middle cerebral artery occlusion.

C16 ($p = 0.004$, $R^2 = 0.52$; $p = 0.02$, $R^2 = 0.35$); C20 ($p = 0.05$, $R^2 = 0.29$; $p = 0.007$, $R^2 = 0.47$); C24 ($p = 0.01$, $R^2 = 0.43$; $p = 0.02$, $R^2 = 0.35$); C24:1dh ($p = 0.008$, $R^2 = 0.49$; $p = 0.01$, $R^2 = 0.48$). For the following ceramide and dihydro-ceramide species a significant time-dependent increase could only be shown after 3 h of tMCAO: C14 ($p = 0.02$, $R^2 = 0.36$); C16dh ($p = 0.003$, $R^2 = 0.5$), C24dh ($p = 0.05$, $R^2 = 0.27$). For C18dh a significant linear time-dependent increase could not be shown.

Further analyses focused on sphinganine, a direct precursor of dihydro-ceramide in the *de novo* pathway and sphingosine, a direct precursor of ceramide in the salvage pathway: Sphinganine showed a significant increase 24 h after 60 min of tMCAO. Whereas, a longer duration (180 min) of tMCAO led to a significant decrease of sphinganine 24 h after cerebral ischemia in comparison with a shorter duration (60 min) of tMCAO [Figure 3(a)]. The concentration of sphingosine gradually decreased along with the duration of cerebral ischemia in a 12, 24 and 72 h period after tMCAO with significant values 12 h after tMCAO [Figure 3(b)].

Focal cerebral ischemia leads to impaired glucose tolerance in the OGTT

Blood glucose concentration was measured at the indicated time points before and after oral glucose administration. Fasting blood glucose concentration (time point 0) did not differ significantly compared with the sham group (data not shown).

Cerebral ischemia led to impaired glucose tolerance in an occlusion time-dependent manner: 180 min of tMCAO resulted in long lasting and significantly higher blood glucose concentrations in the OGTT conducted 24 h after the induction of ischemia in comparison with the sham-operated control mice. For 60 min of tMCAO a definite trend towards higher blood glucose concentrations could be shown, however without significant values (Figure 4). At 12 h post-ischemia, blood glucose levels in the tMCAO groups in comparison with the sham-operated groups did not differ (data not shown).

Timing of the pharmacological intervention with propranolol and FTY720

To evaluate the impact of the pharmacological interventions on ischemic lesion size, functional outcome, blood glucose, systemic immune cell counts, and brain tissue ceramide levels and a 24 h observation window was chosen, since a relevant impairment of blood glucose homeostasis could be observed at this time point.

Treatment with FTY720 but not with propranolol reduced circulating blood leukocytes

As expected, FACS analysis documented the rapid effect of FTY720 on systemic leukocyte counts revealing a strong reduction of B-cells, CD4⁺ and CD8⁺ lymphocytes at the time point 24 h after tMCAO (Supplemental Figure 1) corresponding to the sequestration of circulating immune cells in the lymphoid organs as the key mechanism of action of FTY720. In contrast

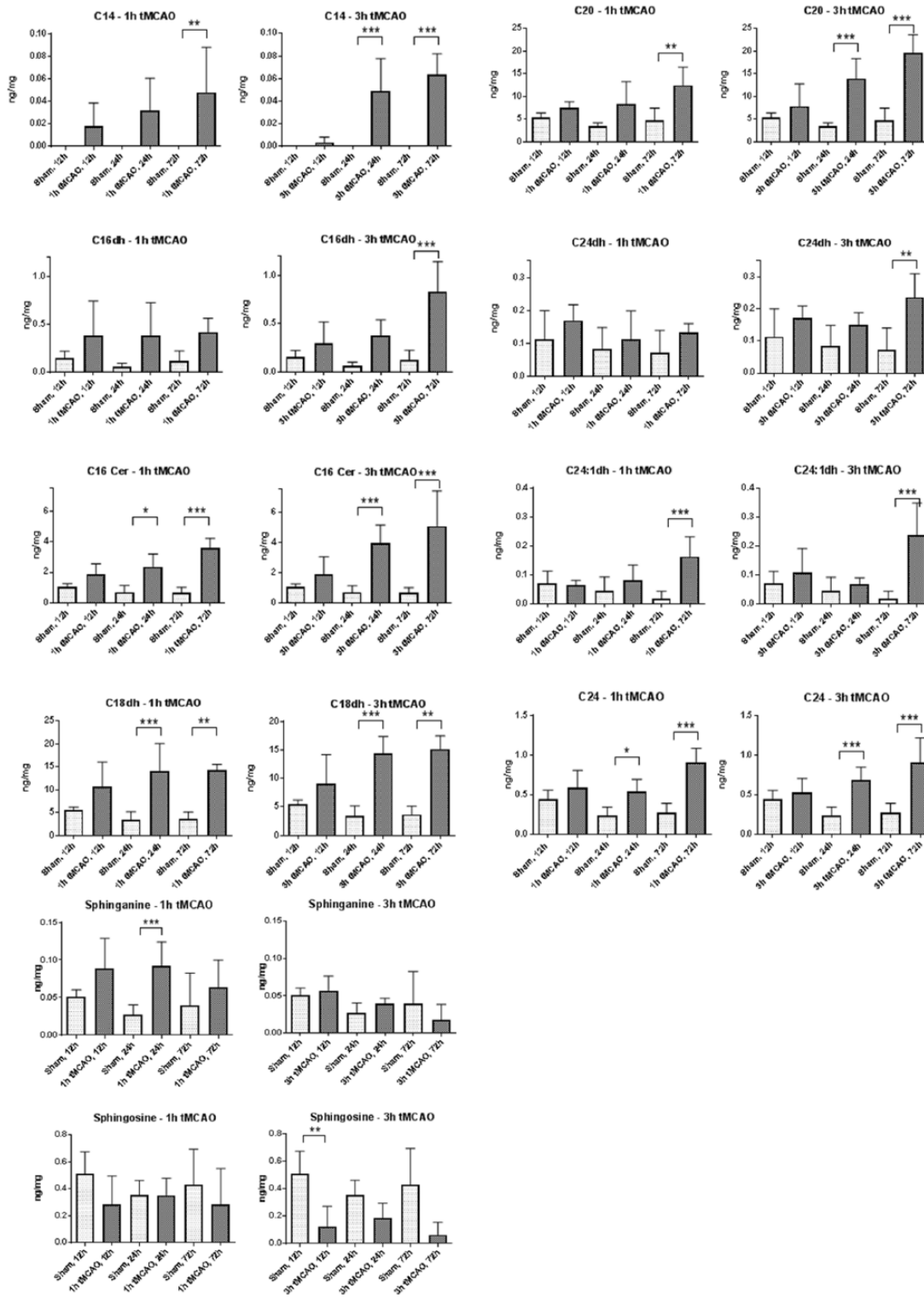


Figure 2. Concentrations of different ceramide species in the ischemic cortex after 1 h or 3 h of tMCAO at the time points 12 h, 24 h and 72 h after tMCAO. The sphingolipid concentrations (ng/mg) determined by LC-MS/MS were related to the wet weight of the brain tissue. The values are the means + SD of $n = 3$ to 7 mice for each group. Statistical significance was assessed with one-way ANOVA and Bonferroni correction. * $p < 0.05$, ** $p < 0.01$, *** $p < 0.001$.

ANOVA, analysis of variance; LC-MS/MS, tandem mass spectrometry; SD, standard deviation; tMCAO, transient middle cerebral artery occlusion.

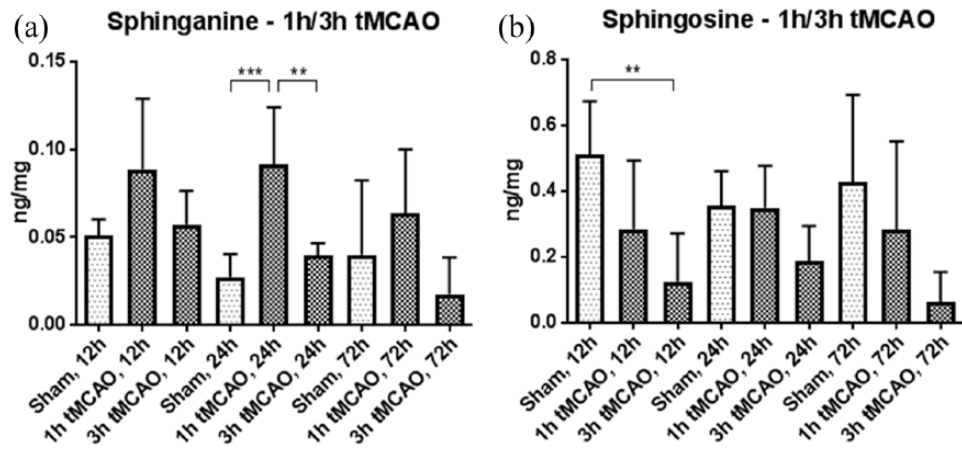


Figure 3. Concentration of sphinganine (a) and sphingosine (b) in the ischemic cortex after 1 h or 3 h of tMCAO at the time points 12 h, 24 h, and 72 h after tMCAO. The sphingolipid concentrations (ng/mg) determined by LC-MS/MS were related to the wet weight of the brain tissue. The values are the means + SD of $n = 3$ to 7 mice for each group. Statistical significance was assessed with one-way ANOVA and Bonferroni correction. ** $p < 0.01$, *** $p < 0.001$. ANOVA, analysis of variance; LC-MS/MS, tandem mass spectrometry; SD, standard deviation; tMCAO, transient middle cerebral artery occlusion.

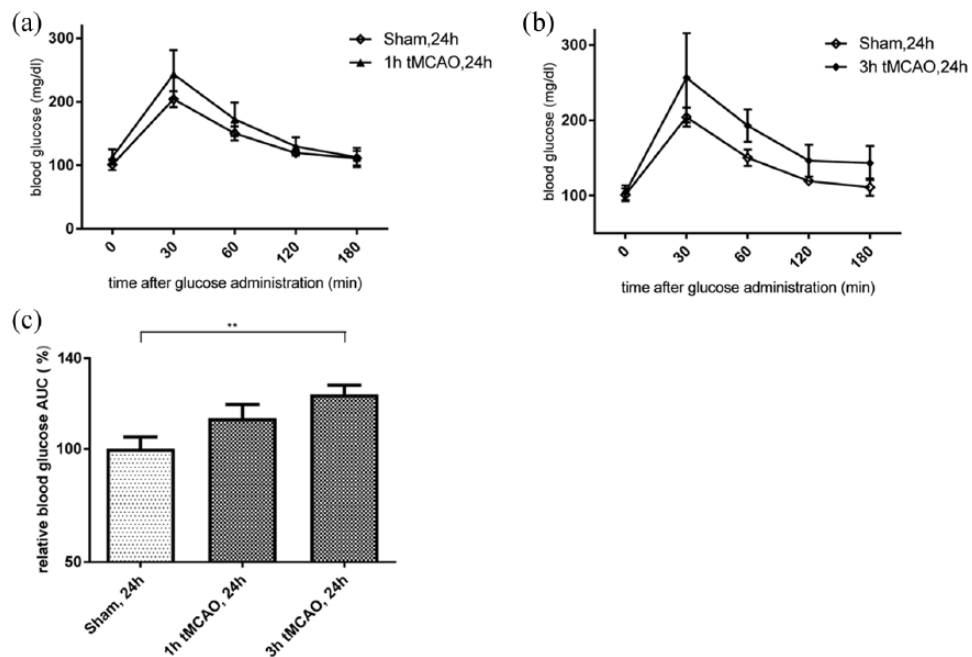


Figure 4. Time course of blood glucose concentration after OGTT conducted 24 h after tMCAO, comparing 1 h of tMCAO (a) and 3 h of tMCAO (b) with the sham-operated control group. The values are the means \pm SD of $n = 5$ to 7 mice for each time point. (c) shows the quantitative evaluation of OGTT results. The area under the curve (AUC) in (a) and (b) was calculated. The values are the means \pm SD. Statistical significance was assessed with one-way ANOVA and Bonferroni correction. ** $p < 0.01$. ANOVA, analysis of variance; AUC, area under the curve; LC-MS/MS, tandem mass spectrometry; OGTT, oral glucose tolerance test; SD, standard deviation; tMCAO, transient middle cerebral artery occlusion.

suppression of the HPN-axis *via* administration of propranolol did not have any effect on the

count of the circulating blood leukocytes in our hands (Supplemental Figure 2).

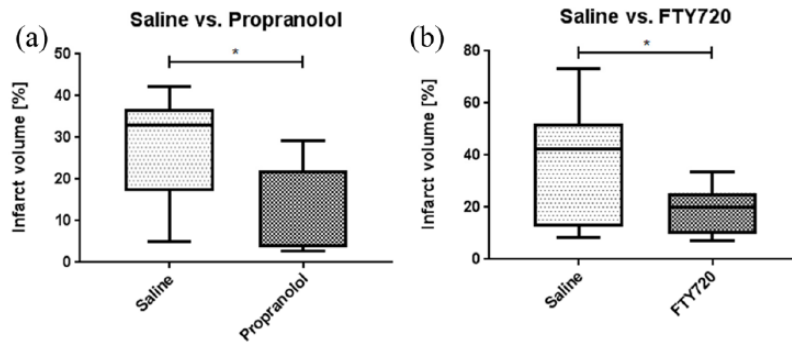


Figure 5. Ischemic lesion size in propranolol-treated (a) FTY720-treated (b) and the respective vehicle-treated control mice with tMCAO of 1 h occlusion time after an observation period of 24 h after tMCAO (propranolol: $n = 7$, vehicle: $n = 9$; FTY720: $n = 8$, vehicle: $n = 10$). The box boundaries mark the 25th and 75th percentile, the line within the box indicates the mean. Whiskers above and below the box mark the minimum and maximum. Statistical significance was assessed with Student's t test, $*p = 0.01$. FTY720, fingolimod; tMCAO, transient middle cerebral artery occlusion.

Treatment with Propranolol and FTY720 both reduced ischemic brain lesion size

Both pharmacological interventions significantly reduced ischemic brain damage [propranolol-treated mice: $11 \pm 4\%$ of contralateral hemisphere, $n = 7$; vehicle-treated mice: $27 \pm 4\%$, $n = 9$, $p = 0.01$, Figure 5(a); FTY720-treated mice: $19 \pm 3\%$ of contralateral hemisphere, $n = 8$; vehicle-treated mice: $37 \pm 7\%$ of contralateral hemisphere, $n = 10$, $p = 0.04$, Figure 5(b)].

Influence of pharmacological interventions on functional outcome after focal cerebral ischemia

Treatment with propranolol improved functional outcome after tMCAO. At 24 h after tMCAO, the median value in the grip test was 4 (range 0–4) in the propranolol-treated mice and 2 (range 1–4) in the saline-treated mice, showing a significant improvement ($p = 0.01$) of neurological outcome. Also in the Bederson score, a trend towards a better functional outcome was obvious, however not statistically significant [median Bederson score: propranolol-treated mice: 3 (range 2–4), saline-treated mice: 1 (range 1–5), $p = 0.06$, Figure 6]. In spite of the significant reduction in infarct volume, the FTY720-treated mice in our study did not show significant functional improvement compared with the saline-treated control group in both neurological assessment tests at the timepoint 24 h after tMCAO [median grip test score: FTY-treated mice: 2.5 (range 0–5), saline-treated mice: 3 (0–5); median Bederson score:

FTY-treated mice: 3 (range 1–5), saline-treated mice: 3 (range 1–5)].

Treatment with propranolol but not with FTY720 decreased ceramide species in the ischemic cerebral cortex after focal cerebral ischemia

Beta-adrenergic antagonism with propranolol decreased several ceramide species in the ischemic cerebral cortex in comparison with the saline-treated control group: A significant reduction was found for C14, C16, C20 and C24 ceramides, as well as for C16-, C18-, C24:1-dihydro-ceramides. In contrast, sphingosine levels were significantly increased in the propranolol-treated group. Concentration of sphinganine in the ischemic cortex was not altered by propranolol treatment (Figure 7). Despite a similar reduction of infarct size, treatment with FTY720 had no significant effect on the concentration of neither of the aforementioned ceramide species in the ischemic cerebral cortex (data not shown).

Treatment with propranolol but not with FTY720 reduced impaired glucose tolerance after focal cerebral ischemia

Blood glucose concentration was measured at the indicated time points before and after oral glucose administration. Treatment with propranolol significantly reduced impaired glucose tolerance caused by cerebral ischemic stress in comparison with the saline-treated group (Figure 8). Fasting blood glucose concentration (time point 0) did not differ significantly compared with the saline-treated group

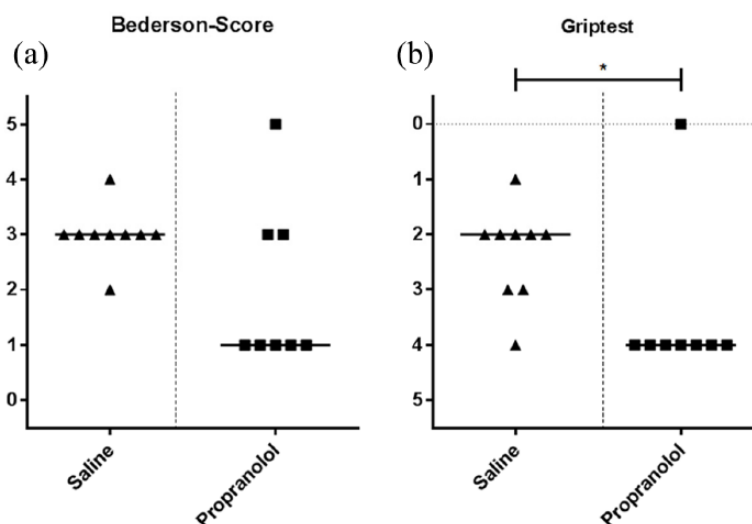


Figure 6. Neurological function was assessed by the Bederson score (a) and grip test (b) in propranolol-treated and vehicle-treated mice 24 h after tMCAO with 1 h occlusion time. The values of single mice and the median are depicted in a dot plot. Statistical significance was assessed with a Mann–Whitney test for two groups. * $p < 0.05$. tMCAO, transient middle cerebral artery occlusion.

(data not shown). Treatment with FTY720 had no significant effect on the development of impaired glucose tolerance (data not shown).

Discussion

The aim of this study was to shed light on a possible interplay between the local ceramide generation in the ischemic brain tissue and stroke-induced glucose intolerance in an animal model of ischemic stroke.

In the first part of our study focusing on alterations of the cerebral sphingolipid metabolism following cerebral ischemia and reperfusion, we found a significant increase of both long chain and very long-chain ceramide species in the ischemic cerebral cortex in comparison with the sham-operated control group. In line with other studies²⁹ investigating healthy brain tissue, long chain ceramide species (C16:0, C18:0, C20:0), were the most abundant in both healthy and ischemic brain tissue. However, not only the temporal dynamics of ceramide accumulation, but also their local tissue composition regarding specific chain lengths and regarding different pathways of ceramide synthesis might influence the biological role of the ceramides. It has already been shown that critical effects of ceramides exerted under physiological conditions but also

in various neurodegenerative and inflammatory diseases are chain length-specific. Ceramide synthases (CerSs) determine chain length of the ceramides and are differentially distributed among tissues;⁷ in the central nervous system C18 ceramide is abundantly produced *via* ceramide synthase 1 (CerS1), which is highly expressed in neurons and essential for normal neuronal development. Ceramide synthase 2 (CerS2) producing C22–C24 ceramides is expressed in oligodendrocytes during myelination.⁸ However, in brain tissue samples from patients with Alzheimer's disease, it could be shown that the amount of long chain ceramides C18:0 and C24:0 contributes to disease severity.³⁰ Moreover, in head and neck squamous cell carcinoma an equipose between C18 ceramide, which is supposed to be a prerequisite of chemotherapy induced apoptosis, and C16, which reduces endoplasmic reticulum stress, hampers apoptosis and is associated with lymphovascular invasion, is an important regulator of cell survival.^{31–33} Regarding the influence of ceramides on inflammatory processes, it could be shown, that an increase in long chain ceramides (C16–C20) in airway epithelium of patients with cystic fibrosis facilitates apoptosis.⁸

Possible pathophysiological links between ceramide metabolism and the induction of apoptosis

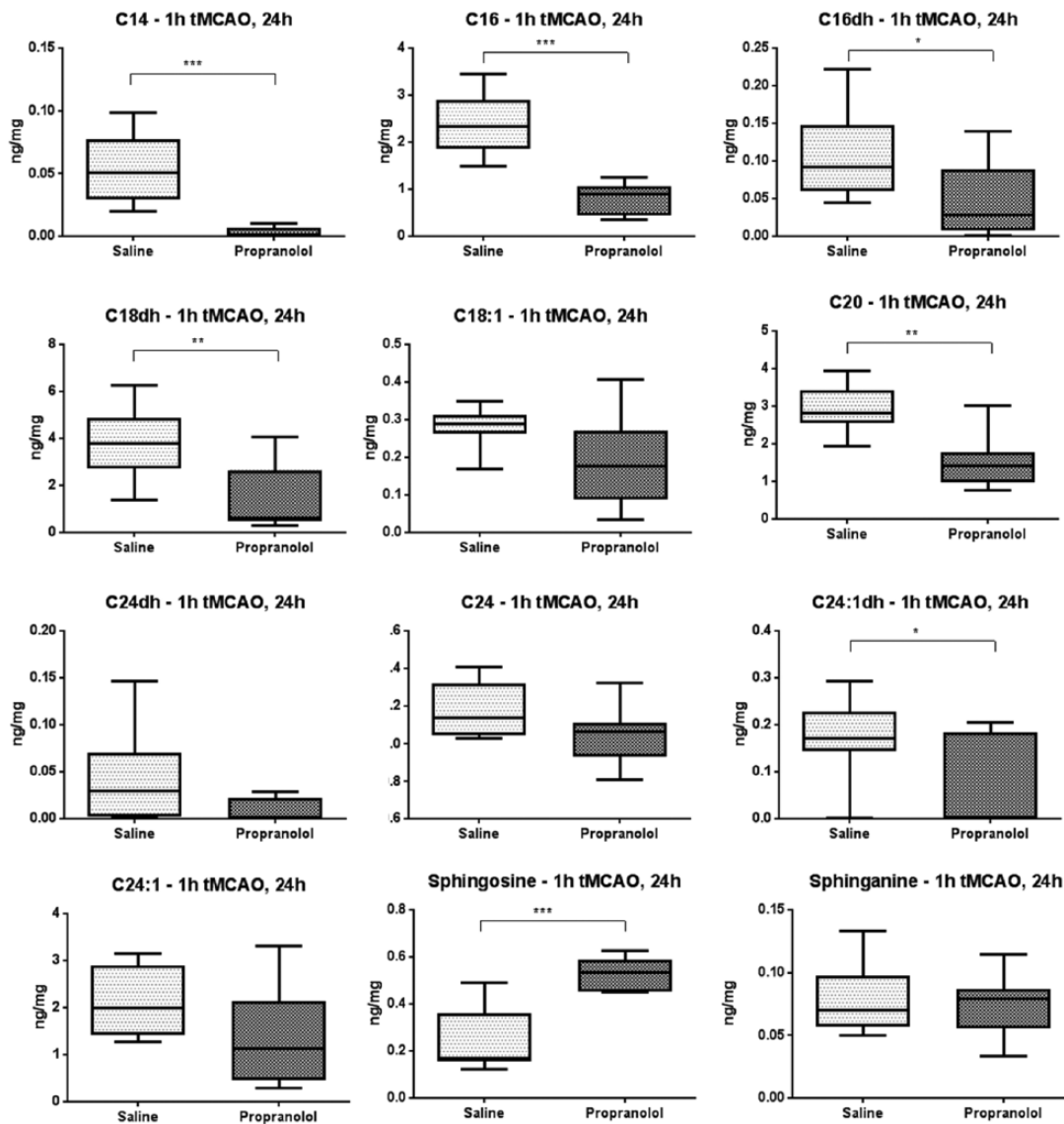


Figure 7. Concentration of different ceramide species in the ischemic cortex after 1 h of tMCAO after an observation period of 24 h after tMCAO in propranolol-treated mice ($n = 7$) in comparison with vehicle-treated control mice ($n = 9$). The sphingolipid concentrations (ng/mg) determined by LC-MS/MS were related to the wet weight of the brain tissue. The values are the means \pm SD. Statistical significance was assessed with Student's *t* test, * $p < 0.05$, ** $p < 0.01$, *** $p < 0.001$.

LC-MS/MS, tandem mass spectrometry; SD, standard deviation; tMCAO, transient middle cerebral artery occlusion.

rely on mitochondrial proteins. The proteins Bak and Bax play a crucial role in the process of the mitochondrial outer membrane permeabilization enabling the release of proapoptotic molecules from the mitochondrial membrane spaces to the cytosol.⁷ It is supposed that Bak triggers ceramide synthesis by binding and activating CerS, consecutively leading to the formation of ceramide-rich macromolecules in mitochondrial membranes and the activation of Bax fostering mitochondrial

outer membrane permeabilization.⁸ It is noteworthy that both the activation of the *de novo* pathway and the activation of the salvage pathway have been described in the context of apoptosis regulation. However, it has to be stressed that not all ceramide species *per se*, irrespective of chain length, induce apoptosis. It is supposed that the equilibrium between long chain and very long chain ceramides determine the cell's fate in the regulation of cell death.³⁴

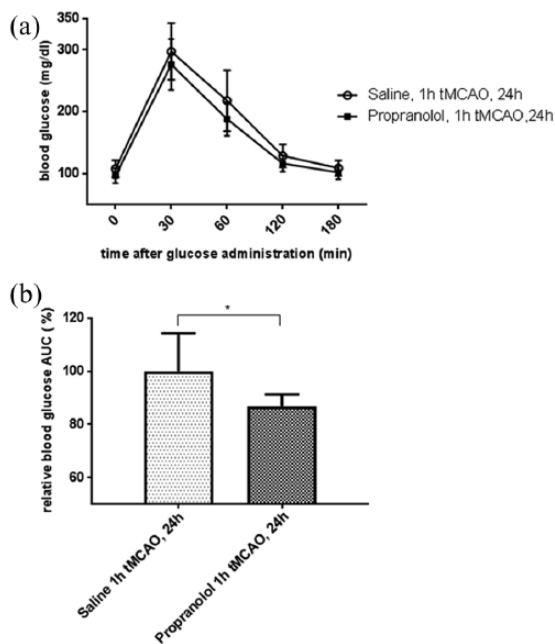


Figure 8. (a) Time course of blood glucose concentration after OGTT conducted 24 h after tMCAO with 1 h occlusion time after treatment with propranolol ($n = 7$) or saline ($n = 9$). The values are the means \pm SD. (b) Quantitative evaluation of OGTT results. The AUC in (a) was calculated. The values are the means \pm SD. Statistical significance was assessed with Student's t test. $*p < 0.05$. AUC, area under the curve; OGTT, oral glucose tolerance test; SD, standard deviation; tMCAO, transient middle cerebral artery occlusion.

In our study, we found an alteration of both long chain (C16:0) and very long chain (C20:0, C24:0) ceramides as well as their respective dihydro-ceramides, precursors in the *de novo* pathway, in the ischemic brain tissue in comparison with the sham-operated controls, suggesting a regulatory role in apoptotic cell death.

Interestingly, C14:0 ceramide was exclusively detectable in the ischemic brain tissue, whereas in the nonischemic control brain samples it was not present at all. C14:0 ceramide is a long chain ceramide, which is mainly synthesized by CerS 5 and 6.³⁵ Previous data suggested that CerS 5 might have a housekeeping function for the synthesis of C14:0 and also C16:0 ceramides as membrane components, since it showed a higher extent of expression in comparison with CerS 6 in different kind of tissues.²⁹ In contrast, CerS 6 may generate lipids under stress conditions, since it is mainly upregulated during apoptotic^{36,37} and inflammatory processes,⁸ both of which occur in ischemic brain damage.

Interestingly, recent studies showed, that certain ceramides might modulate autophagy, a lysosomal pathway which is involved in the turnover of proteins and cellular organelles under stress conditions.⁴ Previous data suggested that C14-ceramide synthesized by CerS 5 is required to induce cardio myocyte autophagy.³⁸ Moreover, in an *in vitro* model it could be shown that experimental knock-down of CerS2 is accompanied by a significant increase in C14:0 and C16:0 ceramides and induces autophagy, while in parallel C24:0 and C24:1 ceramides are significantly downregulated.³⁹ Similarly, experimental induction of autophagy in an experimental model of photo damage is accompanied by an increase in C14:0 and C20:0 ceramides, but in a much lesser extend for C22:0 – C26:0 ceramides, indicating that an equilibrium between long chain and very long chain ceramides is necessary for the regulation of autophagy.⁴⁰ A plausible inductor of autophagy is nutrient deprivation, which is a typical feature of ischemic stress. However, in our experimental study we did not further investigate possible mechanisms of autophagy, therefore it just can be speculated whether the accumulation of C14 ceramide plays a critical role in autophagy regulation in ischemic brain tissue, which is ultimately a protective response of the organism to limit damage under stressful conditions.

Ceramide accumulation in the ischemic brain tissue positively correlated with the time elapsing after transient induction of cerebral ischemia over an observation period of 12, 24 and 72 h. This is in line with previous studies suggesting that the restoration of blood flow to the ischemic tissue, the reperfusion phase, is crucial for the ceramide deposition.⁵ This could be consistently observed in various ischemia/reperfusion *in vivo* models for heart, kidney, lung and also the brain.⁴¹ Therefore, we assume that reperfusion is the key trigger of ceramide generation in our model and that ceramide species accumulate over time in the ischemic brain tissue.

To investigate the relation between ischemic lesion size and ceramide deposition, two different vessel occlusion times (60 min *versus* 180 min tMCAO) were chosen. Whereas a longer tMCAO duration was as expected associated with larger ischemic brain lesions, this did not significantly increase ceramide accumulation, showing that the time elapsed since the initiation of reperfusion and not the severity of the ischemic insult to the brain tissue determined the extent of ceramide production. Interestingly, in our study for

several dihydro-ceramide species (C16dh, C24dh, C18dh) a time-dependent increase was only observed after 3 h of tMCAO but not after a shorter duration of 1 h of ischemia. This may insinuate that also the intensity of ischemia/hypoxia may lead to an increase especially of dihydro-ceramides in the ischemic brain tissue. This finding may be explained by other data, derived from experimental models of hypoxia, where increased levels of dihydro-ceramides were mediated by the inhibition of dihydro-ceramide desaturase 1 (DEGS1) under hypoxic conditions.⁴² The dihydro-ceramide increase was shown to be proportional to the depth and duration of the hypoxic stress.⁴³ Since the desaturase reaction (introduction of double bond) requires oxygen as electron acceptor, hypoxic conditions inhibit DEGS1 activity. Therefore, it was suggested that DEGS1 may act as an oxygen biosensor that modulates ceramide metabolism and that increased dihydro-ceramide levels may act as a hypoxic signal regulating cellular stress responses. Vice versa, increased DEGS1 activity upon reoxygenation (or in our case restoration of blood flow) was supposed to increase ceramide levels and contribute to the deleterious ischemia-reperfusion injury.⁴⁴

Sphinganine, a central precursor of ceramides in the *de novo* pathway, which is further processed to dihydro-ceramides and in a next step desaturated to ceramides, is found to be elevated up to 24 h after 1 h of tMCAO and might indicate that ischemia and reperfusion activate the anabolic *de novo* pathway of ceramide synthesis in the first hours following the insult. However, in the brain lesions induced by 3 h tMCAO, there was no consistent increase of sphinganine at all three observation time points, indicating that the *de novo* pathway may be less active in very severe tissue injury. This is in line with previous experimental findings indicating that mild cerebral ischemia/reperfusion injury causes ceramide accumulation *via* stimulation of mitochondrial ceramide synthase activity rather than from hydrolysis of sphingomyelin.⁴⁵ Vice versa, other data derived from animal experiments showed that ceramide accumulation after lethal cerebral ischemia/reperfusion damage or after chronic cerebral ischemia is due to sphingomyelin hydrolysis *via* activation of acid sphingomyelinases.^{5,46,47}

Sphingosine, which is a precursor of ceramides generated *via* the salvage pathway showed a

tendency to decrease at all three observation time points especially in the brain tissue after 3 h tMCAO in comparison with 1 h tMCAO with the strongest effects early (12 h) after tMCAO. It might be hypothesized that moderate ischemic stress activates the *de novo* pathway upon reperfusion leading to an increase of both sphinganine and ceramide, whereas severe ischemic stress rather impairs the activity of the *de novo* pathway. The fact that the decrease of sphingosine following cerebral ischemia and reperfusion is stronger after a severe tissue insult of 3 h tMCAO as compared with 1 h tMCAO insinuates that following a more severe insult, the ceramide production is then gradually shifted to the salvage pathway, where in the final common path sphingosine is converted to ceramide. Also regarding the salvage pathway, it is suggested that the metabolism of bioactive sphingolipids is highly compartmentalized: complex sphingolipids undergo constitutive degradation in the late endosome and the lysosome-generating ceramide. Lysosomal-generated ceramide cannot leave this cellular compartment unless converted into sphingosine by acid ceramidase. Free sphingosine could be released from the lysosome and consecutively re-acylated by ceramide synthase to ceramide again.⁵ The interconnectivity between the different sphingolipid generating pathways is also documented by several other experimental studies, reporting sphingomyelin hydrolysis and consecutive ceramide accumulation after severe cerebral ischemia/reperfusion damage. These data indicate that cerebral ischemia/reperfusion injury could also trigger sphingolipid recycling *via* the salvage pathway, whereby degradation of complex sphingolipids (glycosphingolipids) produces ceramide and then sphingosine, which is re-acylated to ceramide.^{48,49} However, in contrast with our findings, in the study of Chudakova and colleagues hydrolysis of sphingomyelin in the salvage pathway after severe ischemic stress/reperfusion damage was accompanied by both the accumulation of ceramide and sphingosine in the ischemic brain tissue, highlighting the complexity of sphingolipid signaling.

Summarizing the results of our ceramide profiling of the ischemic brain, it might be hypothesized that moderate ischemic stress activates the anabolic *de novo* pathway of ceramide production, whereas the ceramide generation following a severe insult relies on the salvage pathway. Our findings are in line with previous data, suggesting that the mechanism of ceramide deposition

depends on the severity of the ischemic brain damage.⁵

In the second part of our study focusing on glucose metabolism, we investigated the effect of two licensed drugs, propranolol and FTY720, on stroke-induced glucose intolerance and local ceramide accumulation in the ischemic brain. We found impaired glucose tolerance after tMCAO in line with previously published observations^{14,15} and the clinical observation of the phenomenon of post-stroke hyperglycemia.¹³ The impaired glucose metabolism is not an immediate effect appearing directly after tMCAO, but occurs with a delay shown by a pathological OGTT 24 h after focal cerebral ischemia in comparison with sham-operated control animals. Since the activation of the HPA-axis is one putative pathophysiological mechanism leading to systemic post-stroke hyperglycemia,⁵⁰ one pharmacological intervention with propranolol aimed at blocking the sympathetic nervous system.

As a second pharmacological intervention, we chose to administer the immunomodulatory sphingosine 1-phosphate analog FTY720. In addition to its amply demonstrated neuroprotective and pro-regenerative effects after stroke,^{10–12} recent *in vitro* data suggested that FTY720 also directly blocks ceramide production through inhibition of CerSs.^{21,22}

Both pharmacological interventions significantly reduced ischemic lesion size after experimental stroke in comparison with the vehicle-treated stroke animals. While the neuroprotective effect of FTY720 is well characterized and seems to rely mainly on the lymphocyte depletion induced by this drug,¹¹ it has recently been shown that a combined inhibition of the sympathetic nervous system with propranolol and the HPA axis with mifepristone also reduce ischemic lesion size in the acute phase.⁵¹ While both interventions reduced ischemic lesion size in our experimental setting, only propranolol but not FTY720 significantly improved the stroke-induced impairment of glucose tolerance in comparison with vehicle-treated mice. The fact that both pharmacological interventions reduced ischemic lesion sizes in a standardized mouse model, but only blockage of the HPA axis with propranolol additionally ameliorated glucose utilization, hints at the possibility that the post-ischemic impairment of glucose metabolism is not a metabolic epiphenomenon of a particularly severe

brain damage, but rather an additional (treatable) factor influencing the outcome after ischemic stroke. In addition to the differential effects of these two drugs on glucose metabolism, propranolol also decreased the production and deposition of ceramide species in the ischemic brain tissue in comparison with the saline-treated stroke mice, whereas FTY720 had no relevant influence on ceramide levels in the ischemic brain.

Taking these together, it may be speculated that post-stroke impaired glucose intolerance is a key trigger of cerebral ceramide deposition after ischemic stroke. Thus, on the one hand, suppression of the HPA axis *via* treatment with propranolol abolishes stroke-induced glucose intolerance with consequent reduction of ceramide species in the ischemic cortex. On the other hand, our data suggest that FTY720 exerts its principle effects on reducing infarct growth mainly *via* immunomodulatory mechanisms and without influence on glucose metabolism or direct effects on sphingolipid metabolism. Although it has been shown, that FTY720 (at least *in vitro*) has the potential to inhibit ceramide *de novo* synthesis,^{21,22} in light of our data, it may be speculated that ceramide deposition induced *via* stroke-induced impairment of glucose metabolism is such a strong effect, which cannot be abolished by FTY720's additional 'off-target' effect on ceramide metabolism.

On the basis of these findings, we speculate that there may be a direct link between the severity of the ischemic brain insult and the impaired glucose metabolism on the one hand but also between the systemic metabolic alterations and the cerebral ceramide deposition on the other. This is supported by the finding of a significant increase of cerebral ceramide species in an animal model of diabetes type 1 with streptozotocin-induced severe hyperglycemia.⁵² The authors hypothesized detrimental effects of hyperglycemia-mediated cerebral ceramide deposition, which may constitute an important contribution to hyperglycemia-linked neuro-dysfunction. However, further research is highly warranted to decipher the exact mechanism of pathophysiological connectivity between stroke-induced hyperglycemia and ceramide deposition in the ischemic brain tissue.

However, this experimental study has some limitations that need to be addressed. Due to a relevant drop-out rate, mainly in the groups with long observation time (72 h) and severe cerebral

ischemia (3 h MCAO), the intended sample size was not met in all of the experimental groups, surely affecting the power of the study. This also probably explains, why in the FTY720-treated mice, despite significant decrease in infarct size, we did not find a significant amelioration of the functional neurological deficit.

Since we aimed to set the focus rather on the interplay between post-stroke glucose metabolism and ceramide deposition, we did not perform further expression or activity analyses regarding ceramide generating enzymes (e.g. sphingomyelinases, CerSs), so we can only provide ‘static images’ of cerebral ceramide concentrations at different time points after ischemic brain damage. However, by using LC-MS/MS we used a very reliable technique to measure tissue sphingolipid concentrations and our data are consistent with previous studies investigating ceramide deposition after ischemia/reperfusion tissue damage.

In summary, our data show that stroke-induced glucose intolerance and the accumulation of ceramide species in the ischemic brain tissue occur in parallel.

Both pharmacological interventions, propranolol and FTY720 had positive effects on ischemic lesion size. But only blockade of the sympathetic nervous system by propranolol abolished post-stroke glucose intolerance and reduced post-ischemic cerebral ceramide deposition. Further research regarding the mode of local ceramide deposition in the ischemic brain tissue and the exact interplay with the stroke-induced hyperglycemia is highly warranted.

Acknowledgements

This work was supported by the Fondation Leducq (‘SphingoNet’ consortium) and the SFB1039 (TPB08 to WP and RB). SL was supported by a stipend of the Medical Faculty of the Goethe University in Frankfurt a. M, Germany (‘Patenschaftsmodell’).

Funding

This research received no specific grant from any funding agency in the public, commercial, or not-for-profit sectors.

Conflict of interest statement

The authors declare that there is no conflict of interest.

Supplementary Material

Supplementary material for this article is available online.

ORCID iD

Waltraud Pfeilschifter  <https://orcid.org/0000-0001-6935-8842>

References

1. Truelsen T and Bonita R. The worldwide burden of stroke: current status and future projections. *Handb Clin Neurol* 2009; 92: 327–336.
2. Hannun YA and Obeid LM. Many ceramides. *J Biol Chem* 2011; 286: 27855–27862.
3. Mimeault M. New advances on structural and biological functions of ceramide in apoptotic/necrotic cell death and cancer. *FEBS Lett* 2002; 530: 9–16.
4. Morales A, Lee H, Goni FM, *et al.* Sphingolipids and cell death. *Apoptosis* 2007; 12: 923–939.
5. Novgorodov SA and Gudz TI. Ceramide and mitochondria in ischemic brain injury. *Int J Biochem Mol Biol* 2011; 2: 347–361.
6. Kitatani K, Idkowiak-Baldys J and Hannun YA. The sphingolipid salvage pathway in ceramide metabolism and signaling. *Cell Signal* 2008; 20: 1010–1018.
7. Park WJ and Park JW. The effect of altered sphingolipid acyl chain length on various disease models. *Biol Chem* 2015; 396: 693–705.
8. Grosch S, Schiffmann S and Geisslinger G. Chain length-specific properties of ceramides. *Prog Lipid Res* 2012; 51: 50–62.
9. Shichita T, Ito M and Yoshimura A. Post-ischemic inflammation regulates neural damage and protection. *Front Cell Neurosci* 2014; 8: 319.
10. Czech B, Pfeilschifter W, Mazaheri-Omrani N, *et al.* The immunomodulatory sphingosine 1-phosphate analog FTY720 reduces lesion size and improves neurological outcome in a mouse model of cerebral ischemia. *Biochem Biophys Res Commun* 2009; 389: 251–256.
11. Kraft P, Gob E, Schuhmann MK, *et al.* FTY720 ameliorates acute ischemic stroke in mice by reducing thrombo-inflammation but not by direct neuroprotection. *Stroke* 2013; 44: 3202–3210.
12. Brunkhorst R, Kanaan N, Koch A, *et al.* FTY720 treatment in the convalescence period improves functional recovery and reduces reactive

- astrogliosis in photothrombotic stroke. *PLoS One* 2013; 8: e70124.
13. Fuentes B, Castillo J, San Jose B, *et al.* The prognostic value of capillary glucose levels in acute stroke: the GLyemia in Acute Stroke (GLIAS) study. *Stroke* 2009; 40: 562–568.
 14. Harada S, Fujita WH, Shichi K, *et al.* The development of glucose intolerance after focal cerebral ischemia participates in subsequent neuronal damage. *Brain Res* 2009; 1279: 174–181.
 15. Harada S, Fujita-Hamabe W and Tokuyama S. Ischemic stroke and glucose intolerance: a review of the evidence and exploration of novel therapeutic targets. *J Pharmacol Sci* 2012; 118: 1–13.
 16. Fabian RH and Kent TA. Hyperglycemia accentuates persistent “functional uncoupling” of cerebral microvascular nitric oxide and superoxide following focal ischemia/reperfusion in rats. *Transl Stroke Res* 2012; 3: 482–490.
 17. Robbins NM and Swanson RA. Opposing effects of glucose on stroke and reperfusion injury: acidosis, oxidative stress, and energy metabolism. *Stroke* 2014; 45: 1881–1886.
 18. Won SJ, Tang XN, Suh SW, *et al.* Hyperglycemia promotes tissue plasminogen activator-induced hemorrhage by increasing superoxide production. *Ann Neurol* 2011; 70: 583–590.
 19. Huang NC, Wei J and Quast MJ. A comparison of the early development of ischemic brain damage in normoglycemic and hyperglycemic rats using magnetic resonance imaging. *Exp Brain Res* 1996; 109: 33–42.
 20. Gray CS, Hildreth AJ, Sandercock PA, *et al.* Glucose-potassium-insulin infusions in the management of post-stroke hyperglycaemia: the UK Glucose Insulin in Stroke Trial (GIST-UK). *Lancet Neurol* 2007; 6: 397–406.
 21. Berdyshev EV, Gorshkova I, Skobeleva A, *et al.* FTY720 inhibits ceramide synthases and up-regulates dihydrosphingosine 1-phosphate formation in human lung endothelial cells. *J Biol Chem* 2009; 284: 5467–5477.
 22. Lahiri S, Park H, Laviad EL, *et al.* Ceramide synthesis is modulated by the sphingosine analog FTY720 via a mixture of uncompetitive and noncompetitive inhibition in an Acyl-CoA chain length-dependent manner. *J Biol Chem* 2009; 284: 16090–16098.
 23. Pfeilschifter W, Bohmann F, Baumgarten P, *et al.* Thrombolysis with recombinant tissue plasminogen activator under dabigatran anticoagulation in experimental stroke. *Ann Neurol* 2012; 71: 624–633.
 24. Prass K, Meisel C, Hoflich C, *et al.* Stroke-induced immunodeficiency promotes spontaneous bacterial infections and is mediated by sympathetic activation reversal by poststroke T helper cell type 1-like immunostimulation. *J Exp Med* 2003; 198: 725–736.
 25. Bederson JB, Pitts LH, Tsuji M, *et al.* Rat middle cerebral artery occlusion: evaluation of the model and development of a neurologic examination. *Stroke* 1986; 17: 472–476.
 26. Chen J, Sanberg PR, Li Y, *et al.* Intravenous administration of human umbilical cord blood reduces behavioral deficits after stroke in rats. *Stroke* 2001; 32: 2682–2688.
 27. Friedlander F, Bohmann F, Brunkhorst M, *et al.* Reliability of infarct volumetry: its relevance and the improvement by a software-assisted approach. *J Cereb Blood Flow Metab* 2017; 37: 3015–3026.
 28. Vutukuri R, Brunkhorst R, Kestner RI, *et al.* Alteration of sphingolipid metabolism as a putative mechanism underlying LPS-induced BBB disruption. *J Neurochem* 2018; 144: 172–185.
 29. Schiffmann S, Birod K, Mannich J, *et al.* Ceramide metabolism in mouse tissue. *Int J Biochem Cell Biol* 2013; 45: 1886–1894.
 30. Cutler RG, Kelly J, Storie K, *et al.* Involvement of oxidative stress-induced abnormalities in ceramide and cholesterol metabolism in brain aging and Alzheimer’s disease. *Proc Natl Acad Sci U S A* 2004; 101: 2070–2075.
 31. Karahatay S, Thomas K, Koybasi S, *et al.* Clinical relevance of ceramide metabolism in the pathogenesis of human head and neck squamous cell carcinoma (HNSCC): attenuation of C(18)-ceramide in HNSCC tumors correlates with lymphovascular invasion and nodal metastasis. *Cancer Lett* 2007; 256: 101–111.
 32. Koybasi S, Senkal CE, Sundararaj K, *et al.* Defects in cell growth regulation by C18:0-ceramide and longevity assurance gene 1 in human head and neck squamous cell carcinomas. *J Biol Chem* 2004; 279: 44311–44319.
 33. Senkal CE, Ponnusamy S, Rossi MJ, *et al.* Role of human longevity assurance gene 1 and C18-ceramide in chemotherapy-induced cell death in human head and neck squamous cell carcinomas. *Mol Cancer Ther* 2007; 6: 712–722.
 34. Hartmann D, Lucks J, Fuchs S, *et al.* Long chain ceramides and very long chain ceramides have opposite effects on human breast and colon

- cancer cell growth. *Int J Biochem Cell Biol* 2012; 44: 620–628.
35. Ben-David O and Futerman AH. The role of the ceramide acyl chain length in neurodegeneration: involvement of ceramide synthases. *Neuromolecular Med* 2010; 12: 341–350.
 36. Novgorodov SA, Chudakova DA, Wheeler BW, *et al.* Developmentally regulated ceramide synthase 6 increases mitochondrial Ca²⁺ loading capacity and promotes apoptosis. *J Biol Chem* 2011; 286: 4644–4658.
 37. Schiffmann S, Ziebell S, Sandner J, *et al.* Activation of ceramide synthase 6 by celecoxib leads to a selective induction of C16:0-ceramide. *Biochem Pharmacol* 2010; 80: 1632–1640.
 38. Russo SB, Baicu CF, Van Laer A, *et al.* Ceramide synthase 5 mediates lipid-induced autophagy and hypertrophy in cardiomyocytes. *J Clin Invest* 2012; 122: 3919–3930.
 39. Spassieva SD, Mullen TD, Townsend DM, *et al.* Disruption of ceramide synthesis by CerS2 down-regulation leads to autophagy and the unfolded protein response. *Biochem J* 2009; 424: 273–283.
 40. Separovic D, Kelekar A, Nayak AK, *et al.* Increased ceramide accumulation correlates with downregulation of the autophagy protein ATG-7 in MCF-7 cells sensitized to photodamage. *Arch Biochem Biophys* 2010; 494: 101–105.
 41. Novgorodov SA and Gudz TI. Ceramide and mitochondria in ischemia/reperfusion. *J Cardiovasc Pharmacol* 2009; 53: 198–208.
 42. Siddique MM, Li Y, Chaurasia B, *et al.* Dihydroceramides: from bit players to lead actors. *J Biol Chem* 2015; 290: 15371–15379.
 43. Devlin CM, Lahm T, Hubbard WC, *et al.* Dihydroceramide-based response to hypoxia. *J Biol Chem* 2011; 286: 38069–38078.
 44. Rodriguez-Cuenca S, Barbarroja N and Vidal-Puig A. Dihydroceramide desaturase 1, the gatekeeper of ceramide induced lipotoxicity. *Biochim Biophys Acta* 2015; 1851: 40–50.
 45. Yu J, Novgorodov SA, Chudakova D, *et al.* JNK3 signaling pathway activates ceramide synthase leading to mitochondrial dysfunction. *J Biol Chem* 2007; 282: 25940–25949.
 46. Nakane M, Kubota M, Nakagomi T, *et al.* Lethal forebrain ischemia stimulates sphingomyelin hydrolysis and ceramide generation in the gerbil hippocampus. *Neurosci Lett* 2000; 296: 89–92.
 47. Ohtani R, Tomimoto H, Kondo T, *et al.* Upregulation of ceramide and its regulating mechanism in a rat model of chronic cerebral ischemia. *Brain Res* 2004; 1023: 31–40.
 48. Chudakova DA, Zeidan YH, Wheeler BW, *et al.* Integrin-associated Lyn kinase promotes cell survival by suppressing acid sphingomyelinase activity. *J Biol Chem* 2008; 283: 28806–28816.
 49. Kubota M, Narita K, Nakagomi T, *et al.* Sphingomyelin changes in rat cerebral cortex during focal ischemia. *Neurol Res* 1996; 18: 337–341.
 50. Wang YY, Lin SY, Chuang YH, *et al.* Adipose proinflammatory cytokine expression through sympathetic system is associated with hyperglycemia and insulin resistance in a rat ischemic stroke model. *Am J Physiol Endocrinol Metab* 2011; 300: E155–E163.
 51. Romer C, Engel O, Winek K, *et al.* Blocking stroke-induced immunodeficiency increases CNS antigen-specific autoreactivity but does not worsen functional outcome after experimental stroke. *J Neurosci* 2015; 35: 7777–7794.
 52. Car H, Zendzian-Piotrowska M, Prokopiuk S, *et al.* Ceramide profiles in the brain of rats with diabetes induced by streptozotocin. *FEBS J* 2012; 279: 1943–1952.

Visit SAGE journals online
journals.sagepub.com/
home/tan

 SAGE journals